

PROOF COVER SHEET

Author(s): Jorge E. Valdés

Article title: Proton energy loss in multilayer graphene and carbon nanotubes

Article no: GRAD1442464

Enclosures: 1) Query sheet
2) Article proofs

Dear Author,

1. Please check these proofs carefully. It is the responsibility of the corresponding author to check these and approve or amend them. A second proof is not normally provided. Taylor & Francis cannot be held responsible for uncorrected errors, even if introduced during the production process. Once your corrections have been added to the article, it will be considered ready for publication.

Please limit changes at this stage to the correction of errors. You should not make trivial changes, improve prose style, add new material, or delete existing material at this stage. You may be charged if your corrections are excessive (we would not expect corrections to exceed 30 changes).

For detailed guidance on how to check your proofs, please paste this address into a new browser window: <http://journalauthors.tandf.co.uk/production/checkingproofs.asp>

Your PDF proof file has been enabled so that you can comment on the proof directly using Adobe Acrobat. If you wish to do this, please save the file to your hard disk first. For further information on marking corrections using Acrobat, please paste this address into a new browser window: <http://journalauthors.tandf.co.uk/production/acrobat.asp>

2. Please review the table of contributors below and confirm that the first and last names are structured correctly and that the authors are listed in the correct order of contribution. This check is to ensure that your name will appear correctly online and when the article is indexed.

Sequence	Prefix	Given names(s)	Surname	Suffix
1.		Juan D.	Uribe	
2.		Mario	Mery	
3.		Bernardo	Fierro	
4.		Raul	Cardoso-Gil	
5.		Isabel	Abril	
6.		Rafael	Garcia-Molina	
7.		Jorge E.	Valdés	
8.		Vladimir A.	Esaulov	

Queries are marked in the margins of the proofs, and you can also click the hyperlinks below. Content changes made during copy-editing are shown as tracked changes. Inserted text is in **red font** and revisions have a red indicator . Changes can also be viewed using the list comments function. To correct the proofs, you should insert or delete text following the instructions below, but **do not add comments to the existing tracked changes**.

AUTHOR QUERIES

General points:

- (1) **Permissions:** You have warranted that you have secured the necessary written permission from the appropriate copyright owner for the reproduction of any text, illustration, or other material in your article. Please see <http://journalauthors.tandf.co.uk/permissions/usingThirdPartyMaterial.asp>.
- (2) **Third-party content:** If there is third-party content in your article, please check that the rightsholder details for re-use are shown correctly.
- (3) **Affiliation:** The corresponding author is responsible for ensuring that address and email details are correct for all the co-authors. Affiliations given in the article should be the affiliation at the time the research was conducted. Please see <http://journalauthors.tandf.co.uk/preparation/writing.asp>.
- (4) **Funding:** Was your research for this article funded by a funding agency? If so, please insert ‘This work was supported by <insert the name of the funding agency in full>’, followed by the grant number in square brackets ‘[grant number xxxx]’.
- (5) **Supplemental data and underlying research materials:** Do you wish to include the location of the underlying research materials (e.g. data, samples or models) for your article? If so, please insert this sentence before the reference section: ‘The underlying research materials for this article can be accessed at <full link>/ description of location [author to complete]’. If your article includes supplemental data, the link will also be provided in this paragraph. See <<http://journalauthors.tandf.co.uk/preparation/multimedia.asp>> for further explanation of supplemental data and underlying research materials.
- (6) The **CrossRef database** (www.crossref.org/) has been used to validate the references. Mismatches will have resulted in a query.

QUERY NO.	QUERY DETAILS
AQ1	Please check and confirm that the affiliations of the authors have been set correctly.
AQ2	Please check and confirm that the author names have been set correctly.
AQ3	Please note that the Funding section has been created by summarising information given in your acknowledgements. Please correct if this is inaccurate.

AQ4	The funding information provided (Basal Program for Centers of Excellence) has been checked against the Open Funder Registry and we failed to find a match. Please check and resupply the funding details.
AQ5	The funding information provided (CEDENNA) has been checked against the Open Funder Registry and we failed to find a match. Please check and resupply the funding details.
AQ6	The funding information provided (CONICYT) has been checked against the Open Funder Registry and we found a partial match with “CONICYT”. Please check and resupply the funding details.
AQ7	one should put the energies here & for reference 6.
AQ8	add reference.
AQ9	Please spell out “CVD” at its first mention in the text.
AQ10	If it is in the middle of the bond it is not maximum also.
AQ11	Please spell out “TRIM” at its first mention in the text.
AQ12	The disclosure statement has been inserted. Please correct if this is inaccurate.
AQ13	The CrossRef database (www.crossref.org/) has been used to validate the references. Mismatches between the original manuscript and CrossRef are tracked in red font. Please provide a revision if the change is incorrect. Do not comment on correct changes

How to make corrections to your proofs using Adobe Acrobat/Reader

Taylor & Francis offers you a choice of options to help you make corrections to your proofs. Your PDF proof file has been enabled so that you can edit the proof directly using Adobe Acrobat/Reader. This is the simplest and best way for you to ensure that your corrections will be incorporated. If you wish to do this, please follow these instructions:

1. Save the file to your hard disk.
2. Check which version of Adobe Acrobat/Reader you have on your computer. You can do this by clicking on the “Help” tab, and then “About”.

If Adobe Reader is not installed, you can get the latest version free from <http://get.adobe.com/reader/>.

3. If you have Adobe Acrobat/Reader 10 or a later version, click on the “Comment” link at the right-hand side to view the Comments pane.

4. You can then select any text and mark it up for deletion or replacement, or insert new text as needed. Please note that these will clearly be displayed in the Comments pane and secondary annotation is not needed to draw attention to your corrections. If you need to include new sections of text, it is also possible to add a comment to the proofs. To do this, use the Sticky Note tool in the task bar. Please also see our FAQs here: <http://journalauthors.tandf.co.uk/production/index.asp>.

5. Make sure that you save the file when you close the document before uploading it to CATS using the “Upload File” button on the online correction form. If you have more than one file, please zip them together and then upload the zip file.

If you prefer, you can make your corrections using the CATS online correction form.

Troubleshooting

Acrobat help: <http://helpx.adobe.com/acrobat.html>

Reader help: <http://helpx.adobe.com/reader.html>

Please note that full user guides for earlier versions of these programs are available from the Adobe Help pages by clicking on the link “Previous versions” under the “Help and tutorials” heading from the relevant link above. Commenting functionality is available from Adobe Reader 8.0 onwards and from Adobe Acrobat 7.0 onwards.

Firefox users: Firefox’s inbuilt PDF Viewer is set to the default; please see the following for instructions on how to use this and download the PDF to your hard drive: http://support.mozilla.org/en-US/kb/view-pdf-files-firefox-without-downloading-them#w_using-a-pdf-reader-plugin



Proton energy loss in multilayer graphene and carbon nanotubes

Juan D. Uribe^a, Mario Mery^a, Bernardo Fierro^a, Raul Cardoso-Gil^{a,b}, Isabel Abril^c, Rafael Garcia-Molina^d, Jorge E. Valdés^a and Vladimir A. Esaulov^{a,e}

^aDepartamento de Física, Laboratorio de Colisiones Atómicas, Universidad Técnica Federico Santa María, Valparaíso, Chile; ^bPlanck-Institut für Chemische Physik fester Stoffe, Dresden, Germany; ^cDepartament de Física Aplicada, Universitat d'Alacant, Alacant, Spain; ^dDepartamento de Física – Centro de Investigación en Óptica y Nanofísica, Universidad de Murcia, Murcia, Spain; ^eInstitut des Sciences Moléculaires d'Orsay, Université Paris Saclay, Orsay, France

Q1
Q2

ABSTRACT

Results of a study of electronic energy loss of low keV protons interacting with multilayer graphene targets are presented. Proton energy loss shows an unexpectedly high value as compared with measurements in amorphous carbon and carbon nanotubes. Furthermore, we observe a classical linear behavior of the energy loss with the ion velocity but with an apparent velocity threshold around 0.1 a.u., which is not observed in other carbon allotropes. This suggests low dimensionality effects which can be due to the extraordinary graphene properties.

ARTICLE HISTORY

Received 22 December 2017
Accepted 5 February 2018

1. Introduction

The use of the interaction of energetic particles with solid matter is a useful tool in fundamental areas of physics and technological applications in material science, biomedicine, nuclear and space industry, material characterization and new spectroscopies applied to nano-science (1). Particle interaction with nanostructures is one of the most interesting phenomena, where the crucial parameter to study is the amount of deposited energy and how it is transferred to the media. Nowadays, the emergence of true possibilities to obtain ultrathin films allows us to study the phenomena of electronic excitations by energetic ions at very low energies. New research on flat nanostructures, such as graphene (2,3), presents extensive possibilities to study their extraordinary physical and chemical properties under different configurations and environments, including radiation exposure.

Graphene is emerging as one of the most attractive materials for particle sieving including gases, liquids and other kind of molecules. A recent review of graphene-based membranes covers these topics (4). Graphene in a pristine state is impermeable to almost all thermal atoms and molecules, especially hydrogen and helium under ambient conditions (4–6). On the other hand, particles with high kinetic energy can pass through graphene layers, but interacting with highly dense electron cloud, transfer much more energy to graphene

CONTACT Jorge E. Valdés  jorge.valdes@usm.cl; Vladimir A. Esaulov  vladimir.esaulov@u-psud.fr

47 than to bulk systems (6). This conclusion is supported by the recent **time-dependent den-**
Q7, 48 **sity functional theory** (TD-DFT) calculations. For energetic ions, like proton and helium, the
49 transferred energy per unit path length through electronic excitations turns out to be at
50 least twice as high as that corresponding to graphite and amorphous carbon (7–9).

51 The kinetic energy, charge state and trajectories of the particles are affected in a different
52 manner by materials which have a well-differentiated electronic and crystalline structure.
53 For particles at energies less than 10 keV, these interactions play a significant role in sput-
54 tering, ion implantation and in various characterization techniques (e.g. Low Energy Ion
55 Scattering-LEIS), in which particles probe the first few atomic layers of nanostructured mate-
56 rials (10,11). In the energy range considered in this work, experimental data on the stopping
57 cross section in any material is very scarce and deserves to be studied to extend tests of the
58 reliability of theoretical models and semi-empirical data compilations (12,13). These results
59 which may present considerable differences with bulk results deserve to be investigated.

60 In this progress report, we discuss experimental measurements of the electronic energy
61 loss of proton beams transmitted through multilayer graphene (MLG) films. The proton inci-
62 dent energy range goes from 1 to 10 keV. To our knowledge, there exists no other similar
63 data on such a material, to which our experiments could be compared. Hence, we com-
64 pare our experiments with data obtained for protons in amorphous carbon and nanotubes
Q8, 65 obtained in our laboratory and abroad. In the Figure 1, we show a sketch of our experiment
66 where ions interact with graphene and nanotubes.

68 2. Experiment

70 2.1. Sample description

71 We obtained a set of commercial samples from the Graphenea company (14). Briefly, as
72 the company claims, graphene layers were synthesized by CVD method on a Cu substrate.
Q9, 73 The MLG films were prepared by transferring and stacking independently 10 (10) graphene
74 layers on a user requested substrate, in a multiple transfer procedure (non-AB Bernal config-
75 uration). In our case, all samples were transferred onto Quantifoil gold TEM grid substrates
76 (15) and suspended over 2 μm holes. The transfer procedure of these samples follows the
77 method described in the work of Ochoa et al. (16) and patented by Graphenea. The nomi-
78 nal thickness of these films is 3.45 nm, considering that the theoretical graphene thickness
79 is 0.345 nm. Raman analysis of the stacked graphene layers shows spectra characteristic of
80 graphene, which means *the layers are not interacting among themselves*. The same result was
81 obtained recently by Chen et al. in fabricating two stacked monolayers (17).

84 2.2. Energy loss measurements

85 To determine the electronic energy loss, we use the transmission geometry, where ions pass
86 through very thin self-supported films, with thicknesses preferably less than 20 nm, which
87 are less than the proton penetration depth in our low energy range. A brief description of
88 the experimental arrangement is given hereafter. Multilayer graphene samples are placed
89 in front of the beam with a five-axis precision manipulator. The operating pressure in the
90 ion gun system is 5×10^{-4} Pa and the energy loss measurements were performed in the
91 collision chamber with a pressure around of 4×10^{-6} Pa.
92

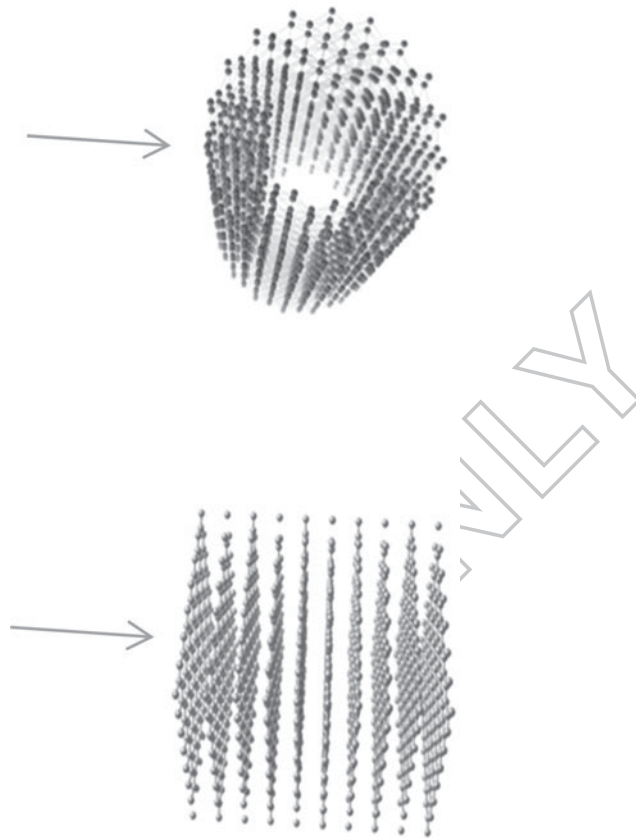


Figure 1. Sketch of the experiment. Ion beam hitting MLG and MWCNT targets.

Ions are generated by a Colutron hot discharge source (18), then accelerated, focused, and mass and charge selected, to obtain protons with energies in the range of 1 to 10 keV. To avoid damage to the samples, a common practice in this kind of experiment is to diminish to a minimum value the ion beam current, which is reduced to obtain fluencies less than 6×10^9 protons/cm². The proton energy is measured using a spherical sector electrostatic energy analyzer with a resolution of less than 1% at FWHM. Protons are detected using multichannel plates MCP in a Chevron configuration. Ions entering the analyzer were detected with an angular acceptance of 0.5°, at 0° and at 3° with respect to the ion beam direction. Detection at 3° is used to avoid an overlap of the incident energy distribution with that coming from the target and used to prevent excessive bombardment of the MCP detectors located at 0°. This overlapping is due to the presence of pinholes in the sample, allowing passage of the incident beam.

In Figure 2, we show the energy distributions for protons after passing through the MLG target, measured at 0° (blue full circles) and 3° (red empty circles). The incident energy was 5 keV. A slight difference in energy is observed which is due to possible path length enlargements caused by the effect of multiple scattering phenomena. The nuclear loss is neglected due to the small scattering angles with respect to the incident direction. Roughly speaking,

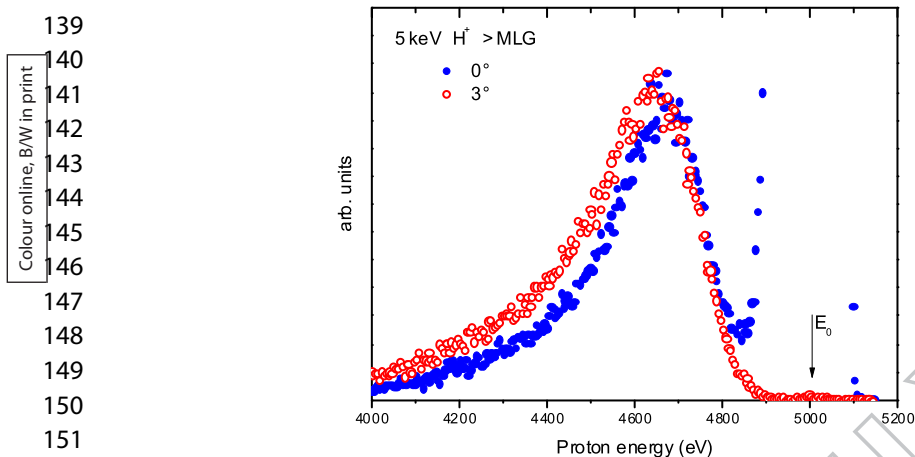


Figure 2. This plot shows energy distributions of transmitted protons through the MLG target. These distributions were measured at 0° (blue full circles) and 3° (red empty circles), with respect to the incident direction, with an angular acceptance of 0.5° . The incident beam, indicated by an arrow at 5000 eV, passes through pinholes in the target and its energy distribution overlaps with the right wing of the proton distribution coming from the target. Elastic loss, or nuclear stopping power, is negligible in this case.

passage through 10 layers of carbon means an estimated nuclear loss of 20 eV at 3° with protons at 5 keV (12). We consider that these differences fall within the experimental error. We can observe that the present energy distributions show large tails at the lower energy side in contrast to the energy distributions observed in metallic films which have a Gaussian-like shape (19). To evaluate the proton electronic energy loss, we use the most probable energy in the energy distribution (peak position) and the energy loss, in eV/A, is calculated using the nominal thickness of MLG sample, which corresponds to 3.45 nm. The uncertainty in our energy measurements has been minimized and it is less than 1%, which is equivalent to 10–20 eV.

3. Experimental results and discussion

Figure 3 shows the most probable electronic energy loss, in eV/A, as a function of the proton velocity (in atomic units) for protons interacting with carbon allotropes. Red symbols correspond to our measurements on MLG targets. Our results show a linear behavior as a function of velocity, with a surprising and not expected feature, an apparent velocity threshold merge at 0.1 a.u. (250 eV) velocity. Another interesting characteristic is that the proton energy loss in MLG is larger as compared with the values obtained for amorphous carbon and nanotubes (12,13,20,21). The isolated point at 0.63 a.u. (10 keV) corresponds to a test measurement to verify linearity. In between 5 and 10 keV, we did not perform measurements, in order to avoid target damage. For comparative purposes, we include data for protons energy loss in amorphous carbon (blue symbols), obtained from data compilations (13). Also shown are the experimental energy losses for protons in carbon nanotubes of different dimensions. Green symbols correspond to proton energy loss data in a multi-wall carbon nanotube with an internal diameter of 5 nm and an external diameter of 27 nm, which correspond to a wall thickness 11 nm (20). Black symbols correspond to

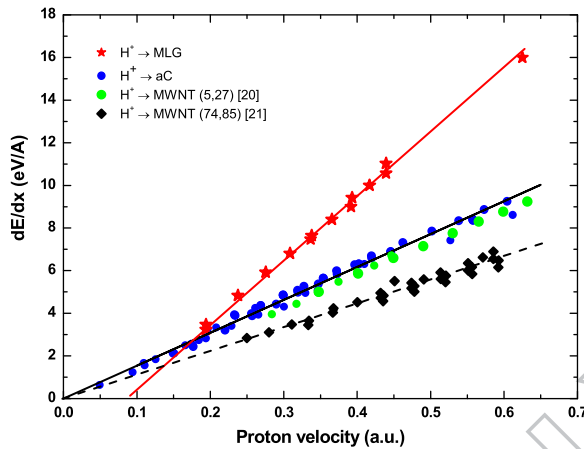


Figure 3. Proton electronic energy loss in $\text{eV}/\text{\AA}$ as a function of ion velocity in a.u. Exhibited data correspond to targets of graphene multilayers (MLG), amorphous carbon and nanotubes, for two different dimensions, see text. The dotted lines are given to guide the eye to the intercept point of the linear extrapolation. Red symbols correspond to our measurements. Blue symbols are proton energy losses in amorphous carbon (13). Green and black symbols correspond to proton energy loss in MWCNT nanotubes, see text (20,21).

proton energy loss data in nanotubes with an internal diameter of 74 nm and an external diameter of 85 nm, corresponding to a wall thickness of 5.5 nm (21). In the case of amorphous carbon and carbon nanotubes, we observe a linear behavior for the energy loss, as a function of proton velocity, with different slopes.

Our experimental results are compared with recent *ab initio* calculations. These approaches combine classical molecular dynamics and TD-DFT to describe proton interaction with graphene (7,8). Their study is focused on the energy transfer to graphene when protons travel perpendicular to the hexagonal structure of graphene in two specific points, in the middle of the C–C bond and in the middle of the hexagon. A common feature of their results is the large energy per unit path length transferred to graphene in the energy range of our experiment and the non-linearity of energy loss as a function of velocity. The energy loss as a function of the incident energy (see Figure 4) turns out to be highest for passage between the middle of the C–C bond.

In Figure 5, we repeat part of the information appearing in Figure 3. In this plot, we show a comparison between our experiment and theory. To compare our experiment with the mentioned theories, we take the energy transfer value, corresponding to a single graphene layer as given by those calculations. We multiply that energy transfer by the number of layers of the MLG and then divided by the total thickness of the target, which is 34.5 Å. Symbols in Figure 5 are blue symbols (up and down triangles) correspond to calculations made by Bubin et al. (8), where up triangles correspond to energy transferred by the proton to electrons belonging to the C–C bond and would correspond to the maximum particle energy loss in Figure 4. Down triangles would correspond to the minimum energy loss due to the low electron density present in the hexagon. Red symbols are the same as in Figure 3. Black symbols correspond to calculations performed by Krashennnikov (7) and have the same meaning as the blue ones. Also shown in Figure 5, for reference, a black line indicates

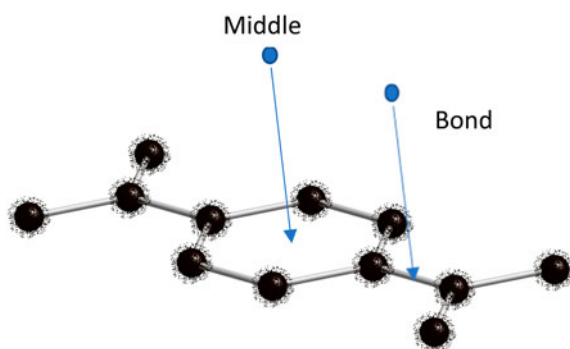


Figure 4. Sketch of proton interaction with graphene used in the theoretical approaches (7,8).

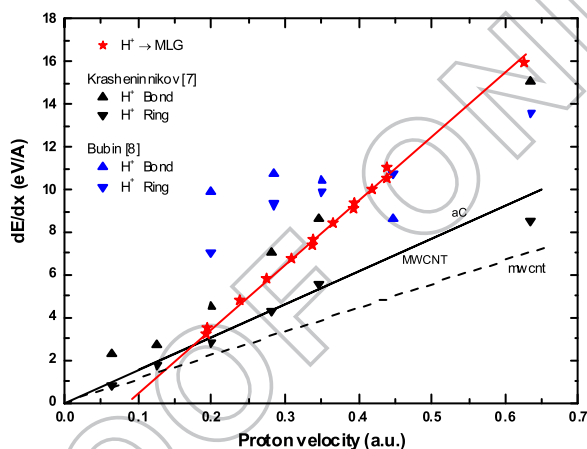


Figure 5. Proton electronic energy loss in $\text{eV}/\text{\AA}$ as a function of ion velocity in a.u. For comparison with our measurements, we include data from recent theoretical calculations, which combine both classical molecular dynamic and time-dependent density functional theory. Blue data correspond to data from ref. (8) and black symbols correspond to data calculated in the same framework, ref. (7), see text for detailed explanation of symbols. The red line is the linear approximation to our experimental data. The amorphous carbon data are approximated by a black solid line, which also represent, approximately, data obtained from the MWCNT (5,22), see Figure 3.

proton energy loss in amorphous carbon. Both calculations indicate that the energy losses in graphene should be higher than in amorphous carbon. Our experimental data appear to lie close to the high limit (middle C–C bond) of the energy losses, predicted by reference (7) and, the ring center contribution to energy loss, which corresponds to the lowest electron density region, agree with the amorphous carbon data.

Despite similar methods of calculations, there are significant differences between results of the two theoretical but discussion of these approaches is beyond the scope of this work. However, both theories agree in their prediction of high energy transfer to graphene by energetic protons.

While the higher energy loss trend of the experimental data agrees on the whole with the indications of theory that the energy losses in graphene are higher than in amorphous carbon, one also needs to consider other possible reasons such as contaminations. There are

277 different sources of contamination one can consider. These are water molecule and hydro-
278 carbon adsorption, and also some residual PMMA in transferring graphene layers. The work
279 of Ochoa et al. (16), on which the Graphenea samples are based, suggests that the main con-
280 taminant should be water. Their model of a graphene multilayer derived from a detailed
281 spectroscopic ellipsometry study and XPS includes a circa 1.1 nm effective interlayer thick-
282 ness of a contamination layer consisting predominantly of water and traces of the other
283 contaminants. Based on this, using the semi-empirical calculations from Ziegler (12), we
284 can estimate the contribution of 1.1 nm of mainly water to the energy loss at 5 Å to be 35 eV.
285 This would reduce the energy loss protons in Figure 3 and 5 by 0.35 eV/Å, which would still
286 result in a significantly higher energy loss than that of amorphous carbon.

287 Note also that F. Mao et al. (9), using TD-DFT, also predict high energy losses for He₂⁺ inter-
288 acting with graphene layers, reaching three times the results obtained by Echenique et al.
289 (23). For instance, for helium ions at 1 keV (0.1 a.u. of velocity), the energy loss in graphene
290 predicted for by F. Mao is around 11 eV/Å, meanwhile, Echenique gives 3.3 eV/Å. Also,
291 recent experiments of slow highly charged ions interacting with graphene layers report
292 that the energy loss and charge exchange of ions in two-dimensional materials show sig-
293 nificant differences with respect to bulk solids (24,25). The high energy losses differ by an
294 order of magnitude with respect to results obtained by TRIM (12).

295 The higher energy loss for protons, found in our experiments and which recent calcula-
296 tions would fairly explain, can be traced to the unusual properties of graphene. Assuming
297 that the measured energy loss is due to electronic excitations, and graphene with a high
298 electron mobility can react very fast to the presence of the intruder, near the surface, with its
299 subsequent fast screening (25). This phenomenon produces a very high and fast flux of elec-
300 trons against the energetic proton producing a high momentum transfer which translates
301 into a high graphene stopping power on the particle.

302 Another interesting feature appearing in our experiments is the apparent velocity
303 threshold in the protons energy loss, which appears around 0.1 a.u. of velocity (see Figure 5).
304 From the theoretical point of view, calculations of stopping power at low energies in the
305 frame of the free electron gas model, using linear response theory, non-linear DFT and the
306 transport cross section model (22,26), predict that the stopping power is linear with the ion
307 velocity. However, experiments show that this prediction is not necessarily true for protons
308 and helium in metals and insulators. For instance, the predicted proportionality with the ion
309 velocity of the stopping power of transition metals (Cu, Ag and Au) for protons breaks down
310 drastically at some very low velocities displaying two well-differentiated regimes (27). This
311 phenomenon is explained considering the existence of a threshold effect for electron-hole
312 pair excitation, where the valence electrons in these materials, mainly non-free *d* electrons,
313 need a minimum of energy to be excited. Recently, this phenomenon of non-linearity with
314 the ion velocity has been studied with TD-DFT calculations (28), obtaining a more realistic
315 description of stopping power for H and He in metals like Au. This work finds very good
316 quantitative agreement with experiments, describing the deviation from the ion velocity
317 proportionality.

318 In the case of large band-gap insulators, such as LiF and KCl, a threshold effect was found
319 for protons, deuterium and helium ions. Data obtained indicated a velocity threshold of
320 around 0.1 a.u., below which particles pass through the material without energy loss, i.e.,
321 no electron excitations. For insulators, the electron excitations are suppressed due to a
322 minimum excitation energy, the energy band gap of these materials plays a fundamental

323 role. The interaction of low energy protons, in these cases, was described by invoking the
324 creation of negative ions and charge interchange via electron promotion (29–33).

325 In the case of protons interacting with graphene at low energies, there may be sufficient
326 time for successive charge transfer, leading to negative ion formation as this occurs on, e.g.
327 graphite (34), in which case it is a negative ion and not a fast proton passing through a high
328 electron density cloud, which could then affect the scattering process and energy loss.

329 This work deserves to be extended to the case of different numbers of graphene layers in
330 the target. We consider this work as a starting point to study several low dimensional struc-
331 tures under particle irradiation and its effect on particles dynamics. These interesting results
332 might be used in technological applications in nanostructures material characterization,
333 radiation protection, ‘solar protons cells’ in space energy storage.

334 **Acknowledgements**

336 V. E. acknowledges the hospitality of the Physics Department at UTFSM.

337 **Disclosure statement**

339 No potential conflict of interest was reported by the authors.

340 **Funding**

342 This work was mainly supported by the grants Fondecyt [grant number 1100759], CONICYT-MEC
343 [grant number 80150073] and DGIIIP-UTFSM grant. Also, MM and BF acknowledge to Basal Program
344 for Centers of Excellence, Grant FB0807 CEDENNA, CONICYT.

345 **References**

- 347
348
349 (1) Hellborg, R.; Whitlow, H.J.; Zhang, Y. Eds. *Ion Beam in Nanoscience and Technology*; Springer-
350 Verlag: Berlin and Heidelberg, 2009.
- 351 (2) Novoselov, K.S.; Geim, A.K.; Morozov, S.V.; Jiang, D.; Katsnelson, M.I.; Grigorieva, I.V.; Dubonos,
352 S.V.; Firsov, A.A. *Nature* **2005**, *438*, 197.
- 353 (3) Castro Neto, A.H.; Novoselov, K. *Rep. Prog. Phys.* **2011**, *74*, 082501.
- 354 (4) Li, H.; Song, Z.; Zhang, X.; Huang, Y.; Li, S.; Mao, Y.; Ploehn, H.J.; Bao, Y.; Yu, M. *Science* **2013**, *342*,
355 95.
- 356 (5) Liu, G.; Jin, W.; Xu, N. *Chem. Soc. Rev.* **2015**, *4*, 2026.
- 357 (6) Hu, S.; Lozada-Hidalgo, M.; Wang, F.C.; Mishchenko, A.; Schedin, F.; Nair, R.R.; Hill, E.W.;
358 Boukhvalov, D.W.; Katsnelson, M.I.; Dryfe, R.A.W., et al. *Nature* **2014**, *516*, 227.
- 359 (7) Krashennnikov, A.V.; Miyamoto, Y.; Tomanek, D. *Phys. Rev. Lett.* **2007**, *99*, 016104.
- 360 (8) Bubin, S.; Wang, B.; Pantelides, S.; Varga, K. *Phys. Rev. B.* **2012**, *85*, 235435.
- 361 (9) Mao, F.; Zhang, C.; Gao, C.-Z.; Dai, J.; Zhang, F.-S. *J. Phys. C: Condens. Matt.* **2014**, *26*, 085402.
- 362 (10) Bracco, G.; Holst, B., Eds. *Surface Science Techniques*; Springer-Verlag: Berlin and Heidelberg, 2013.
- 363 (11) Liu, G.; Jin, W.; Xu, N. *Chem. Soc. Rev.* **2015**, *44*, 5016.
- 364 (12) Ziegler, J.F.; Biersack, J.; Littmark, U. *The Stopping and Range of Ions in Solid*, Vol. 1, Pergamon
365 Press: New York, 1985.
- 366 (13) Montanari, C.C.; Dimitriou, P. *Nucl. Instrum. Meth. Phys. Res. B.* **2017**, *408*, 50.
- 367 (14) Graphenea. 2018 – Donostia San Sebastián, Spain, <http://www.graphenea.com>.
- 368 (15) Quantifoil Micro Tools GmbH. www.quantifoil.com, Germany.
- (16) Ochoa-Martínez, E.; Gabás, M.; Barrutia, L.; Pesquera, A.; Centeno, A.; Palanco, S.; Zurutuza, A.;
Algora, C. *Nanoscale* **2015**, *7*, 1491.
- (17) Chen, J.J.; Meng, J.; Yu, D.P.; Liao, Z.-M. *Sci. Rep.* **2014**, *4*, 5065.
- (18) Colutron research Corporation. Boulder, CO, <http://www.colutron.com>.

- 369 (19) Celedón, C.; Sánchez, E.A.; Moreno, M.S.; Arista, N.R.; Uribe, J.D.; Mery, M.; Valdés, J.E.; Vargas, P.
370 *Phys. Rev. A* **2013**, *88*, 137.
- 371 (20) Valdés, J.E.; Celedón, C.; Segura, R.; Abril, I.; Garcia-Molina, R.; Denton, C.D.; Arista, N.R.; Vargas, P.
372 *Carbon. N. Y.* **2013**, *52*, 137.
- 373 (21) Celedón, C.E.; Cortés, A.; Sánchez, E.A.; Sergio Moreno, M.; Uribe, J.D.; Arista, N.R.; Valdés, J.E. *Eur.*
374 *Phys. J. D.* **2017**, *71*, 64. doi:10.1140/epjd/e2017-70408-4.
- 375 (22) Echenique, P.M.; Nieminen, R.M.; Ashley, J.C.; Ritchie, R.H. *Phys. Rev. A* **1983**, *33*, 897.
- 376 (23) Echenique, P.M.; Nieminen, R.M.; Ritchie, R.H. *Solid. State Commun.* **1981**, *37*, 1083.
- 377 (24) Wilhelm, R.A.; Gruber, E.; Ritter, R.; Heller, R.; Facsko, S.; Aumayr, F. *Phys. Rev. Lett.* **2014**, *112*,
378 153201.
- 379 (25) Gruber, E.; Wilhelm, R.A.; Pétuya, R.; Smejkal, V.; Kozubek, R.; Hierzenberger, A.; Bayer, B.C.;
380 Aldazabal, I.; Kazansky, A.K.; Libisch, F. *Nat. Commun.* **2016**, *7*, 13948. doi:10.1038/ncomms13948.
- 381 (26) Echenique, P.M.; Nieminen, R.M.; Ritchie, R.H. *Solid. State Commun.* **1981**, *37*, 1083.
- 382 (27) Valdés, J.E.; Eckardt, J.C.; Lantschner, G.H.; Arista, N.R. *Phys. Rev. A* **1994**, *49*, 1083.
- 383 (28) Ahsan Zeb, M.; Kohanoff, J.; Sánchez-Portal, D.; Arnau, A.; Juaristi, J.I.; Artacho, E. *Phys. Rev. Lett.*
384 **2012**, *108*, 225504.
- 385 (29) Möller, S.P.; Csete, A.; Ichiola, T.; Knudsen, H.; Uggerhøj, U.I.; Andersen, H.H. *Phys. Rev. Lett.* **2002**,
386 *88*, 193201.
- 387 (30) Serkovic, L.N.; Sánchez, E.A.; Grizzi, O.; Eckardt, J.C.; Lantschner, G.H.; Arista, N.R. *Phys. Rev. A* **2007**,
388 *76*, 040901R.
- 389 (31) Markin, S.N.; Primetzhofer, D.; Bauer, P. *Phys. Rev. Lett.* **2009**, *103*, 113201.
- 390 (32) Souda, R.; Suzuki, T.; Yamamoto, K. *Surf. Sci.* **1998**, *397*, 63.
- 391 (33) Mao, F.; Zhang, C.; Dai, J.; Zhang, F.-S. *Phys. Rev. A* **2014**, *89*, 022707.
- 392 (34) Datta, D.; Shen, J.; Esaulov, V.A. *Nuc. Inst. Meth. Phys. Res. B.* **2013**, *315*, 42.
- 393
- 394
- 395
- 396
- 397
- 398
- 399
- 400
- 401
- 402
- 403
- 404
- 405
- 406
- 407
- 408
- 409
- 410
- 411
- 412
- 413
- 414